Therapeutic Efficacy of Melatonin Pretreated Bone Marrow Mesenchymal Stem Cells Versus Mesenchymal Stem Cells in Experimental Diabetic Cardiomyopathy in Rat

Heba Mohamed Elnegris[1,2], Sahar Khalil[3], Dahlia Badran[4,5] and Rania Galhom[6,7,8]

Original Article

Department of Histology and Cell Biology, Faculty of Medicine, [1]Zagazig University, Zagazig, [2]Badr University in Cairo, Cairo, [3]Suez Canal University, Ismailia, Department of Biochemistry Molecular Biology, Faculty of Medicine, [4]Suez Canal University, Ismailia, [5]Badr University in Cairo, Cairo, Department of Human Anatomy and Embryology, [6]Suez Canal University, Ismailia, [7]Badr University in Cairo, Cairo, [8]Tissue Culture Unit, Center of Excellence in Molecular and Cellular Medicine (CEMCM), Suez Canal University. Ismailia, Egypt

ABSTRACT

Background: Diabetic cardiomyopathy (DCM) is a common condition that is associated with morbidity and mortality. With the medical advancement in cell treatment, stem cell therapy has a potential therapeutic strategy for DCM.

Objectives: We aim to evaluate the possible therapeutic effects of Mesenchymal stem cells (MSCs) versus melatonin (MLT) preconditioned-MSCs in induced diabetic cardiomyopathy in rats.

Materials and Methods: Forty-five male adult albino rats were divided into four groups. Group I: Control group. Group II: Diabetic group: Rats received single intraperitoneal injection of streptozotocin STZ (50 mg/kg body weight). Group III: DC treated with MSCs. Group IV: DC treated with MLT preconditioned-MSCs. Histological, ultrastructural and immunohistochemical studies were performed on left ventricle myocardium. We also estimated the survival of MLT-preconditioned MSCs in vitro. Bcl-2, Casp-3, interleukin 1 (IL-1), and interleukin 10 (IL-10) expression were measured using real-time PCR in tissue homogenates.

Results: Our findings revealed a significant increase in immunohistochemical expression of apoptotic markers in the diabetic group, as well as a disruption of the normal cardiac histological ultrastructure. Melatonin improved MSCs survival in vitro and altered apoptotic markers. In addition, the melatonin-preconditioned MSC group showed a significant increase in B-cell lymphoma 2 (Bcl-2) mRNA expression and a significant decrease in Casp-3. Enhanced immunomodulatory behavior was obvious by a significant attrition of the mRNA expression of IL-1β (inflammatory-agonist) and a significant altitude of IL-10 (inflammatory-antagonist).

Conclusion: The melatonin-preconditioning of MSCs enhance their survival and immunomodulatory activities and precisely restored cardiac histology. Thus, it unveils an encouraging interference of DC.

Key Words: Albino rats, Melatonin, Mesenchymal stem cells, Myocardial, Type II Diabetes mellitus.

Revised: 25 September 2022, **Accepted:** 19 October 2022

Corresponding Author: *Heba Mohamed Elnegris*, *Department of Histology and Cell Biology, Faculty of Medicine, Zagazig University, Zagazig, Egypt,* **Tel.:** *+20552301474*, **E-mail:** *heba.negres@buc.edu.eg.*

ISSN: 1110-0559, December2021, Vol. 5, No. 2.

INTRODUCTION

Diabetic cardiomyopathy (DCM) is a disorder with abnormal myocardial structure and performance occurring in people with diabetes mellitus despite the lack of other cardiac risk factors and is associated a poor prognosis. Regardless of the convenient state-of-the art therapy as diuretics or heart resynchronization medications, DCM remains a leading edge of morbidity and fatality in diabetics (de Ferranti *et al.* 2014a; Spezzacatene *et al*. 2015). Hence, studying DCM pathogenesis and finding an innovative therapy for treating it is essential.

Data from previous literatures have highlighted an obvious contribution of hyperglycemia in increasing pro-inflammatory cytokines, promoting myocardial inflammation and /or fibrosis (Jia *et al*. 2015; Pan *et al*. 2014). Increased levels of transforming growth factor (TGF)-β, expanded deposition of extracellular matrix proteins (ECM) such as collagen, and activation of cardiac myofibroblasts (Leask 2015), all of which contribute to ventricular rigidity, dilation, and hypertrophy, were attributed for these effects. Subsequently, functional alterations in the form of diastolic deterioration, systolic impairment, and ultimately clinical failure of the heart were recorded (Ni *et al*. 2020a).

 DOI: 10.21608/jmh.2022.165071.1104

MSC cytotherapy is likely a probable innovative avenue for medication of cardiac lesion and for advancement of histological reclamation as they were proved to possess an immunoregulatory, anti-apoptotic, anti-inflammatory, and a secretory function in diabetes and many heart diseases (Williams and Hare 2011; Zhang *et al*. 2017). It was shown that MSCs transplantation in rat model of DCM could downregulate transforming growth factor-β1 (TGF-β1) and (TNF-α) expression, alleviate cardiac fibrosis, consequently, enhances ventricular compliance and cardiac function when being transplanted intravenously (Zhang *et al*. 2017). It was also recorded that intra myocardial injection of MSCs could inhibit cardiomyocyte death, induce angiogenesis and characterization of cardiac progenitor cells after myocardial infarction (Nascimento *et al*. 2014). MSCs were shown to have the same myocardial reparative power when injected intramuscularly through modulating the production and release of numerous tissue repair-related cytokines via paracrine processes (Mao *et al*. 2017).

Various types of autologous stem cell were used in different clinical trial and proved to maintain viable myocardial tissue with adjusted function (Hare *et al*. 2017; Houtgraaf *et al*. 2012). However, despite being a promising therapeutic approach for many heart diseases, this type of therapy still faces many limitations including limited survival of transplanted cells or the risk of in-vivo differentiation to undesirable cell linage. Recent strategies for improving stem cell therapy have focused on enhancing cellular survival pathways and boosting differentiation into efficient cardiomyocytes by preconditioning stem cells with drugs or cytokines (Sano *et al*. 2020). MLT, principally originated by the pineal gland, manifested to have a significant aspect in the adjustment of bone turnover and melatonin deficiency is thought to be associated with several disorders, including insomnia, cancer, and cardiovascular and neurodegenerative diseases (Li *et al*. 2019). It was also reported to have anti-senescence properties and could protect MSCs by increasing the silent information of regulator type 1 (SIRT1), a crucial genetic managing tissue endurance (Zhou *et al*. 2015). Besides, it could increase MSCs resistance of oxidative stress (Chen *et al*. 2022). So, the main intention of this research was to evaluate the therapeutic effectiveness of MSCs versus melatonin preconditioned MSCs (MLT-MSCs) in DCM rat model.

MATERIALS AND METHODS

2.1. Experimental animals and experiment design:

Animals were obtained from and kept at Animal House-Faculty of Medicine, Zagazig University, Egypt. We utilized Forty-five adult male rats (Wistar albino) weighing 185 – 200 g (12 – 14 weeks old). The animals were acclimatized in plastic cages supplied by a stainless-steel wire-bar lid. The temperature was kept at (22 ± 1 °C), also the humidity is managed at (54 ± 5 %). The room was artificially illuminated with (12:12 h light: dark cycle). Their diet was the standard laboratory formula and they had free access to water. The environment was chemically free. All animals were treated in accordance with Zagazig University's Ethical Committee and NIH Guidelines. An acceptance from the local Institutional Animal Care and Use Committee, Zagazig University, Egypt [ZU-IACUC] was obtained, approval number [ZU-IACUC/3/F/1912022/].

Rats were randomly divided into 4 groups, as following:

Group I (control group): containing 15 rats and divided equally into three subgroups:

Subgroup A (1A): (negative control): Rats received no treatment.

Subgroup B (1B): Each rat received a single intra-peritoneal (IP) injection of 0.5 ml sodium citrate buffer (SCB) (pH 4.5); [vehicle of streptozotocin (STZ)].

Subgroup C (1C): Each rat received single injection of 0.5 ml phosphate buffer saline (PBS) [vehicle for Stem Cells] through the tail vein.

The remaining 30 rats were subjected to diabetes induction by injection of a single intraperitoneal injection of STZ (50 mg/kg; Sigma Aldrich, St. Louis, MO, USA) (Mohamed, Reda, and Elnegris 2020). Rats were considered diabetic when their random blood glucose was more than 250 mg/dL for three successive days (Wang *et al.* 2014). The 30 diabetic rats were split equally into three groups, each of 10:

Group II (Diabetic group): received nothing else.

Group III (Diabetic & non-preconditioned MSCs group): Diabetic rats were subjected to transplantation of 5×106 MSCs suspended in 0.5 ml PBS through the tail vein, 12 weeks after the induction of diabetes (Cooney *et al*. 2016; Nascimento *et al*. 2014).

Group IV (Diabetic & melatonin preconditioned MSCs group): Diabetic rats were subjected to transplantation of 5×106 melatonin (1μm) preconditioned MSCs suspended in 0.5 ml PBS (Li *et al*. 2021), through the tail vein, 12 weeks after diabetes induction as group III.

Four weeks after injection of MSCs with or without precondition to melatonin, rats in all groups were anaesthetized with IP injection of ketamine (90 mg/kg)/xylazine (15 mg/kg) then sacrificed (El-Akabawy and El-Kholy 2014). Left ventricles tissue specimens were collected by median incision of thorax. The heart was sectioned transversely at the mid ventricular level. left ventricles myocardial tissue specimens were split into two groups. Specimens of the 1st group were prepared for light microscopic and electron microscopic examination. The 2nd group of specimens was stored at – 80 °C for RNA withdrawal to assess mRNA expression of Bcl-2, casp-3, IL -1β, and IL-10 genes.

2.2. Preparation of STZ and induction of diabetes:

STZ was obtained from Sigma Aldrich, St. Louis, MO, USA as a powder and was prepared by dissolving it in SCB (pH 4.5). Rats were fasted for 8 hours before receiving STZ injection and given water as normal. STZ was given to rats in a single intraperitoneal injection at a dose of 50 mg/kg (Abdollahi *et al*. 2011). Random blood sugar measurements for all rats were performed daily in the Biochemistry Department, Faculty of Medicine, Zagazig University, two days after STZ injection. When the animals' random blood glucose levels exceeded, they were classified as diabetic (Annadurai *et al*. 2012).

2.3. Separation and cultivation of bone marrow-derived mesenchymal stem cells:

For preparing the MSCs, ten (6-weeks old) male albino rats were used. Dulbecco's modified Eagle's medium (DMEM) supplemented with 10 % fetal bovine serum (FBS) was used to flush the tibiae and femurs of the rats to harvest bone marrow. Cells with nuclei were assorted with a density gradient re-cultured in culture medium composed of 89 % DMEM (Lonza, Belgium), 10 % FBS (Seralab, Brazil) and 1 % 1 % penicillin-streptomycin (PS) (1:1) (Lonza, Belgium). After incubation of cells at 37 °C with 5 % humidified CO2 for duration of 2 weeks till production of big colonies (80 – 90 % confluence). Subculture was performed by washing the cells of primary passage (P0) with PBS (Lonza, Belgium) and their splitting from the tissue culture vessel with 0.25 % trypsin in 1 mL EDTA (Gibco, Grand Island, NY) (5 - 10 min at temperature of 37 °C). After completion of centrifugation, re-incubation of cells was done in 50 cm^2 culture flask (Falcon) with serum-added medium and expanded to the 3rd passage (P3). MSCs in culture were identified by their stickiness, colony formation and spindle shape (Soleimani and Nadri 2009).

2.4. Bone marrow mesenchymal stem cell characterization and labeling:

Antibodies against CD 90, 105, 106, and CD11 were used to characterize BM-MSCs by fluorescence activated cell sorting (FACS, NE15106; Beckman Coulter, Brea, CA). According to the proposal of the International Society for Cellular Therapy (ISCT), the immunophenotyping was chosen (Dominici *et al*. 2006). Prior to rat injection, BM-MCs were labeled using the Paul Karl Horan PKH 26 Red Fluorescent Cell Linker Kit for General Cell Membrane Labeling (Sigma, St. Louis, Missouri, USA) (Haas *et al*. 2000). A fluorescent microscope was used to study sections of the left ventricle of the stem cell-treated group (Olympus BX50F4, No. 7M03285, Tokyo, Japan). Sections of the left ventricle of the MSCs group were examined by fluorescent microscope (Olympus BX50F4, No. 7M03285, Tokyo, Japan).

2.5. Methylthiazolyldiphenyl-tetrazolium (MTT) analysis for identification of cell proliferation:

To assess MSCs viability with the most suitable dose of MLT (Sigma Aldrich, St. Louis, Missouri, USA) to be used in this experiment. Samples of MSCs only, MSCs + MLT (1 μm), MSCs + MLT (3 μm), and MSCs + MLT (5 μm) were used. MSCs were placed in 96-well tissue culture dishes, each well contained volume of 100 μL. The incubation period for culture dishes were 10 days. Three wells were assigned for a single sample. In the MTT analysis, the MTT reagent (Trevigen Inc., Gaithersburg, MD, USA) was used (10 μL for each well) and the dish was kept in the incubator for 6 h to help the intracellular reduction of the soluble yellow MTT to the insoluble purple formazan dye. While after by usage of dimethyl sulfoxide (DMSO) reagent as an additive to dissolve the formation of formazan crystals. The sample absorbance was assessed on microplate reader at 550600- nm. Six wells for each

group were used to estimate cell proliferation as correlated with non-preconditioned group as control cells (Zhu *et al*. 2019).

2.6. In-vitro analysis of melatonin impacts on the MSCs:

P3 MSCs that had reached an 80 % confluent growth phase were preconditioned with 1 μm MLT and the MLT-containing medium was replaced every day for three days (Fang *et al*. 2018). The cells were trypsinized after three days of MLT administration to assess Bcl-2 and Casp-3 as apoptotic markers, as well as IL1-ß and IL-10 as immunomodulatory indicators by real-time PCR. Non-preconditioned cells were evaluated in each experiment. Information was collected from six separate experiments. All isolation and culture procedures were done at the Central Research Lab, Faculty of Medicine, Zagazig University.

2.7. Real-time PCR study

2.7.1 Bone marrow mesenchymal stem cell apoptotic and immunomodulatory markers expression

Extraction of total RNA from 1×106 cells was performed using the RNeasy Mini kit (cat no #74104, Qiagen, Hilden, Germany) following the manufacturer's instructions and reverse transcribed using Quantiscript reverse transcriptase (QuantiTect Reverse Transcription Kit, Qiagen, Hilden, Germany). The cDNA products were amplified using quantitative real-time PCR with an ABI PRISM 7000 Sequence Detector System (Applied Bio system step1plus) for analysis of Bcl-2, Casp-3, IL-1β and IL-10 mRNA expression. The reaction mixture was composed of 5 μL SYBR Green master mix (Roche Diagnostics, Burgess Hill Sussex, UK), 0.5 μL primers (10 pmol/L), 2 μL cDNA and 2 μL RNAse-free water (Invitrogen, Carlsbad, California, USA) under the following PCR conditions: one cycle of 95 °C for 10 min followed by 45 cycles of 95 °C for 15s, 60 °C for 20s, and 72 °C for 60s. The expression data was normalized using Glyceraldehyde-3-Phosphate Dehydrogenase (GAPDH) as the housekeeping gene. The findings were calculated and assessed using the 2-ΔΔCT method mentioned by Livac and Schmittgen (Livak and Schmittgen 2001). The primer sequences used are listed in Table 1.

2.7.2. Detection of Bcl-2, Casp-3, IL-1β, and IL-10 mRNA expression in tissue homogenate:

Isolation of total RNA from left ventricle tissue homogenate was done using the RNA Easy kit (Qiagen, Hilden, Germany), according to the manufacturer's instruction. RNA concentration and purity were estimated using Nanodrop (UNICO, UV2000, China). The same conditions of RNA reverse transcription and cDNA amplification by PCR using the GAPDH as the housekeeping gene were applied for mRNA expression of apoptotic and immunomodulatory indicators in cell culture. The sequences of forward (F) and reverse (R) primers are given in Table 1.

Table 1: Primer sequences of studied genes:

	Primer sequence
BCL 2 Gene ID: 12043	F 5'-ATCGCCCTGTGGATGACTGAGT-3' R5'-GCCAGGAGAAATCAAACAGAGGC-3'
Casp-3 Gene ID: P70677	F 5'-GGAAGCGAATCAATGGACTCTGG-3' R 5'-GCATCGACATCTGTACCAGACC-3'
IL-1β Gene ID: AJ535730	F 5'-AGAGCAACATCACCATGCAG-3' R 5'-CAGTGAACGCTCCAGGATTT-3'
IL-10 Gene ID: 16153	F 5'-CACCTTCTTTTCCTTCATCTTTG-3' R 5'-GTCGTTGCTTGTCTCTCCTTGTA-3'
GAPDH Gene ID: 100033452 (reference gene)	F 5'-AGTGCCAGCCTCGTCTCATA-3' R 5'- ATGAAGGGGTCGTTGATGGC-3'

2.8. Histopathological studies

2.8.1. Light microscopic assessment:

I- Histological stains:

Specimens were fixed in 10 % neutral formaldehyde saline, then dehydrated and embedded in paraffin wax. They were cut into 5 μm sections. Finally, they were stained using hematoxylin and eosin (Suvarna *et al.* 2018) and Masson's trichrome stains (Chen, Yu, and Xu 2017).

II- Immunohistochemical Techniques:

TNF-a, an inflammatory cytokine, and Casp-3, an apoptotic marker, were immunohistochemically assessed in left ventricles tissue specimens (Ramos-Vara *et al.* 2008). On charged slides, paraffin-embedded serial sections were deparaffinized. To inhibit endogenous peroxidase, they were kept in 0.1 % hydrogen peroxide for 30 minutes. They were then incubated for one night at 4 °C with mouse anti-TNF- antibody (17 kDa) from Thermo Scientific Co. (Cat #12 - 7321 - 82) and anti-Casp-3 antibody (32 kDa) from Thermo Scientific Co. (Cat # 43 - 7800) (Sanii *et al*. 2012). Primary antibodies were detected after many PBS washes and a half-hour at room temperature incubation with biotinylated goat anti-mouse IgG (Zymed Laboratories; South San Francisco, CA, USA). Sections were incubated with a streptavidin–biotin–peroxidase complex for another 60 min and 3′, 3 Regular-diaminobenzidine-tetrahydrochloride

(DAB–Sigma-Aldrich Chemical Co., St. Louis, USA) was used to visualize the reactions. Counterstaining by Mayer's hematoxylin was done. TNF-α was seen as brown cytoplasmic reaction and Casp-3 appeared as brown cytoplasmic and nuclear reaction in the left ventricular myocardium (Abd El-kader 2019). Tonsil was used as a positive control of Casp-3, and liver was used as a positive control of TNF-α as provided by the manufacturer. For negative control sections, primary antibody was replaced by PBS.

2.8.2. Transmission electron microscopic examination:

Tiny specimens were fixed using 2.5% phosphate buffered glutaraldehyde (pH 7.4), then post-fixed in 1% osmium tetroxide in the same buffer at 4 °C, dehydrated, and installed in epoxy resin. Semithin 1 μm thick sections were stained using 1 % toluidine blue for light microscopic examination. Uranyl acetate and lead citrate were used to stain ultrathin sections (Bancroft & Gamble, 2013). (JEOL JEM-2100) Transmission Electron Microscope (Jeol Ltd., Tokyo, Japan) in the Electron Microscope Research Unit, Faculty of Agriculture, Mansoura University, Egypt was used to examine, and photograph the sections.

2.8.3. Histo-morphometric analysis:

Using the image analyzer computer system Leica Qwin 500 (Leica Ltd., Cambridge, UK) at the Image Analyzing Unit of Pathology Department, Faculty of Dentistry, Cairo University, Egypt, the following morphometric measurements were done:

• Area percentage of collagen fibers in Masson's trichrome stained sections,

• Optical density of TNF-α and Casp-3 proteins,

• Identification and count of PKh-26-tagged MSCs.

All these parameters were assessed in ten nonoverlapping fields in five slides of five different rats from each group. Area percent and optical density were assessed at a magnification of ×400 (Abas and Sabry 2020) and the number of fluorescent tagged MSCs was assessed at a magnification of ×200.

2.9. Statistical study:

All findings were considered as mean ± SD. Statistical assay was accomplished by software of Statistical Package for the Social Sciences (SPSS), version 13.00 (Chicago, Illinois, USA). Statistical significance was decided by one-way analysis of variance for changes between the means of all groups. Unpaired t-test was used to correlate the mean of the number of fluorescent-tagged cells between groups III and IV. The significance between the study groups was tested using Tukey-Kramer post-hoc test. Probability values (P) less than 0.05 were expressed statistically significant, on the other hand P values less than 0.001 were considered highly significant (Emsley, Dunn, and White 2010).

RESULTS

3.1. Serum glucose levels:

The mean of glucose parameters in control rats, group II, group III, and group IV were 94.2 ± 4.5 mg/dL, 325.4 ± 36.7 mg/dL, 320.5 ± 30.6 mg/dL and 319.4 ± 25.5 mg/dL, subsequently. The intake of STZ ensued a significant altitude in serum glucose parameter when compared to control rats ($P < 0.05$) (Figure 1A).

3.2. Morphological characterization of the isolated MSCs:

During P0, the cells showed a heterogeneous appearance (Figure 2A) but during the subsequent passages (P 1 - 3) almost all the cells acquired homogenous fibroblast-like appearance with abundant cytoplasm, vesicular nucleus with multiple nucleoli (Figure 2B and 2C). Three days after seeding, the culture cells showed plastic adherent property, began to exhibit cytoplasmic processes, and developed different sized colonies.

3.3. BM-MSCs identification by flow cytometry analysis:

Phenotypic FACs analysis of the isolated BM-MSCs during P3 showed that most of the isolated BM-MSCs were uniformly positive for specific MSCs surface marker CD 90 and 105. While most of them were negative for CD11 (Figure 2D).

3.4. mRNA expression of apoptotic and immunomodulatory indicators in BM-MSCs using real-time (qRT-PCR) assay:

Significant increase in the expressions of Bcl-2 and IL-10 in MLT-preconditioned cells was noticed as compared to the non-preconditioned one ($P < 0.05$), while the expressions of Casp-3 and IL-1β showed significant decrease in MLT-preconditioned cells when compared to the non-preconditioned one ($P < 0.05$) (Table 2). The mRNA expression of Bcl-2 and IL-10 elevated and the mRNA expression

of Casp-3 and IL-1β decreased significantly in the MLT- preconditioned cell in a dose reliant way ($P < 0.05$).

Table 2: A Table showing relative mRNA expression in MLT-conditioned and unconditioned MCs with variable doses of MLT:

	Untreated BM-MCs	Treated BM-MCs+ MLT (1µm)	Treated BM-MCs+ MLT (3µm)	Treated BM-MCs+ MLT (5µm)
Bcl 2	1 ± 0.03	1.2 ± 0.03#	1.4 ± 0.01#*	1.5 ± 0.02#*&
Casp 3	1 ± 0.01	0.81 ± 0.01#	0.73 ± 0.02#*	0.42 ± 0.01#*&
IL-10	1 ± 0.02	1.12 ± 0.04#	1.41 ± 0.03#*	1.75 ± 0.03#*&
IL-1β	1 ± 0.01	0.9 ± 0.01#	0.83 ± 0.02#*	0.76 ± 0.01#*&

#P < 0.05 as related to untreated BM-MCs
**P < 0.05 as related to BM-MCs + 1 µm MLT*
& P < 0.05 as related to BM-MCs + 3 µm MLT

3.5. Impact of melatonin on MSC survival:

The response of MLT pretreatment of the MSCs was evaluated by MTT assay. There was no cytotoxic evidential effect of MLT on MSCs in all doses in usage (1µm, 3µm, and 5µm). Besides, there is no significant increase of cell survival in MSCs samples treated with MLT in dose-related pattern than MSCs culture alone. Cell survival ratio for MSCs+MLT (1µm), MSCs+MLT (3µm), MSCs+MLT (5µm) and MSCs only was 87.1 ± 1.3, 87.3 ± 1.4, 87.5 ± 1.5 and 73.7 ± 1.5, consequently and $P < 0.05$ by comparing every MLT- predisposed group to the non-predisposed one (Figure1 B). We choose 1µm MLT to be used in this experiment.

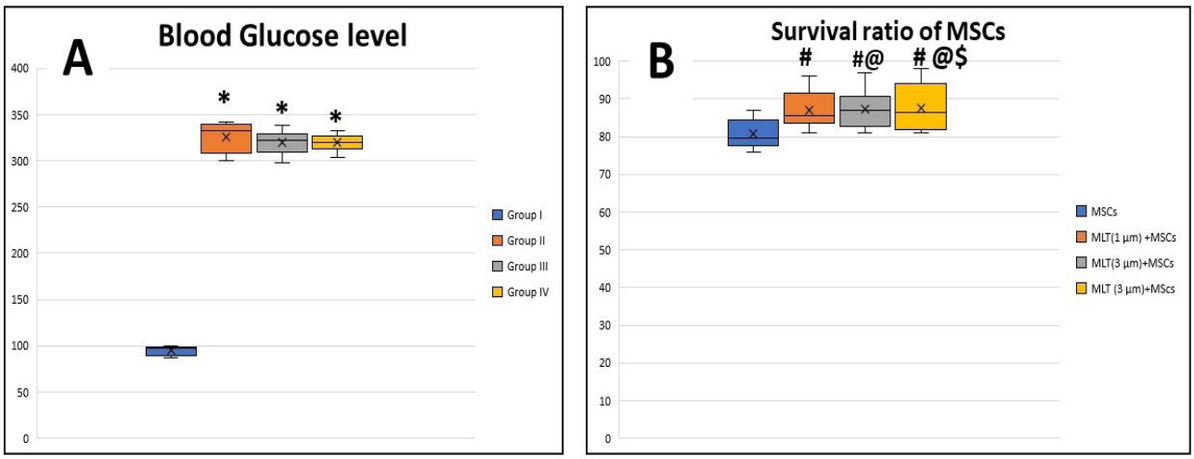

Figure 1: A boxplot chart showing: A) blood glucose level in all rats of all the studied groups. B) Survival ration of nontreated MCs and preconditioned-MCs with different concentrations of MLT. **P < 0.05 as related to group I #P < 0.05 as related to MCs @P < 0.05 as related to MCs + 1 µm MLT $P < 0.05 as related to MCs + 3 µm MLT*

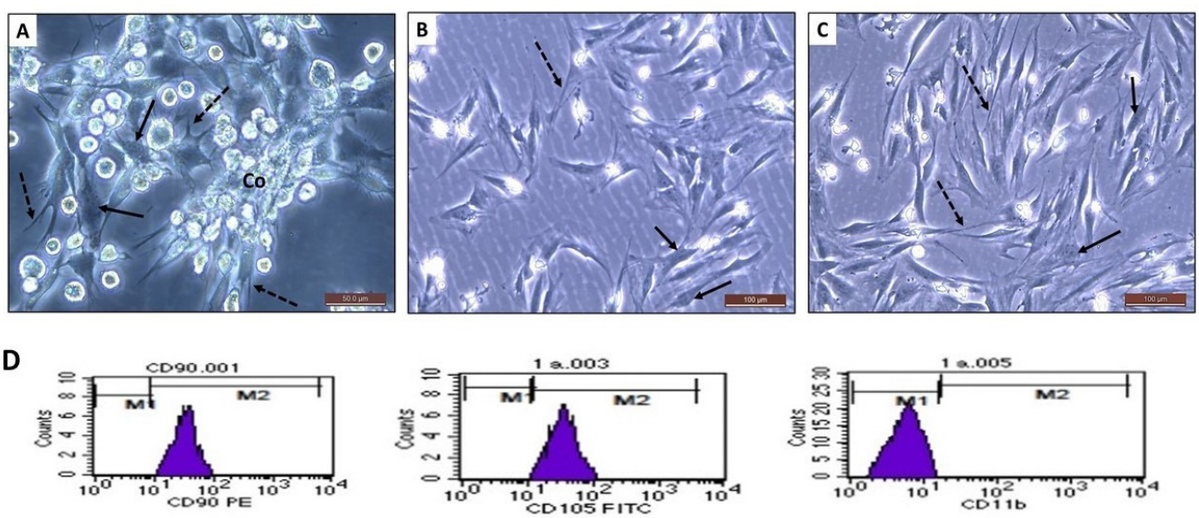

Figure 2: A, B, & C Phase contrast photomicrographs of BM-MCs showing adherent population of cells forming colonies (CO) and exhibited heterogenous morphology during *P*0 (A). The cells acquired homogenous fibroblast-like morphology during *P*1 (B) and *P*3(C). The cells in all passages had vesicular nuclei with multiple nucleoli (arrow) and many cytoplasmic processes (Dashed arrow). D) A phenotypic analysis of different stem markers in the isolated BM-MCs during *P*3.

3.6. Recognition of BM-MSCs homing using fluorescent microscope:

Left ventricular specimens of stem cell-treated rats showed large population of PKH26-tagged MSCs that exposed as brightened red fluorescent spots 4 weeks after MSCs transplantation (Figure 3).

3.7. Histopathological results

3.7.1 Light microscopic examination of H&E-stained sections:

The histological architecture of all subgroups of the control group was similar.

Control group showed regular arrangement of cardiac muscle cells that appeared branching and anastomosing. The cardiac muscle cells showed acidophilic cytoplasm with centrally located oval vesicular nuclei. Intercalated discs were seen at intervals as transverse dark lines, few small capillaries and nuclei of cells belonging to the connective tissue were noticed in the intercellular endomysium spaces (Figure 4a). Diabetic group showed degeneration, fragmentation, and flaring of cardiac muscle cells. Myocardial necrosis, in the form of focal hypereosinophilia, cytoplasmic vacuolization, and peripheral dark nuclei, was detected. There were widening in the tissue spaces with marked inflammatory cellular infiltration. Dilated, congested blood vessels, and extravasated RBCs were also seen (Figure 4b, 4c). MSCs-treated group showed mild preservation of cardiomyocyte morphology and tissue spaces with mild focal necrosis in the form of minimal vacuolization of the cytoplasm. There were few inflammatory cellular infiltrates and no interfibrillar RBCs were found (Figure 4d). Meanwhile, sections of MLT–preconditioned MSCs group showed apparently normal histological picture nearly similar to the control group (Figure 4e).

3.7.2. Light Microscopic examination of Masson's Trichrome-stained sections:

The control group revealed fine blue stained collagen fibers along with the red cardiac muscle cells and in the vicinity of small blood vessels (Figure 5a). The diabetic group revealed obvious increase in the blue stained collagen fibers mainly nearby dilated large blood vessel (Figure 5b). The MSCs-treated group showed moderate collagen fibers deposition between cardiac muscle cells (Figure 5c). The MLT–preconditioned MSCs group showed few amounts of fine blue stained collagen fibers with significant decrease in its area percentage as compared to both diabetes group and MSCs-treated group. Meanwhile, there was non-statistically significant difference when as compared to the control group (Figure 5d). Changes in the mean area percentage of Masson's trichrome-stained sections between all examined rat groups were presented in (Table 3).

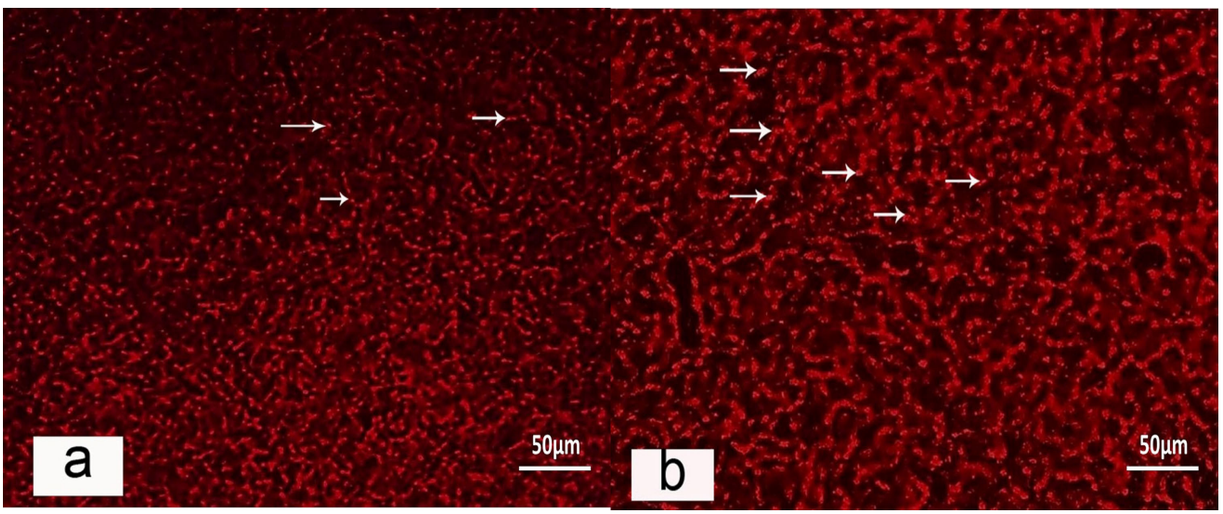

Figure 3: A PKH26-tagged MCs presenting as bright spots (arrows) in (a) mesenchymal stem cell treated group, (b) melatonin conditioned MC group (a, b X200, scale bar = 50 µm)

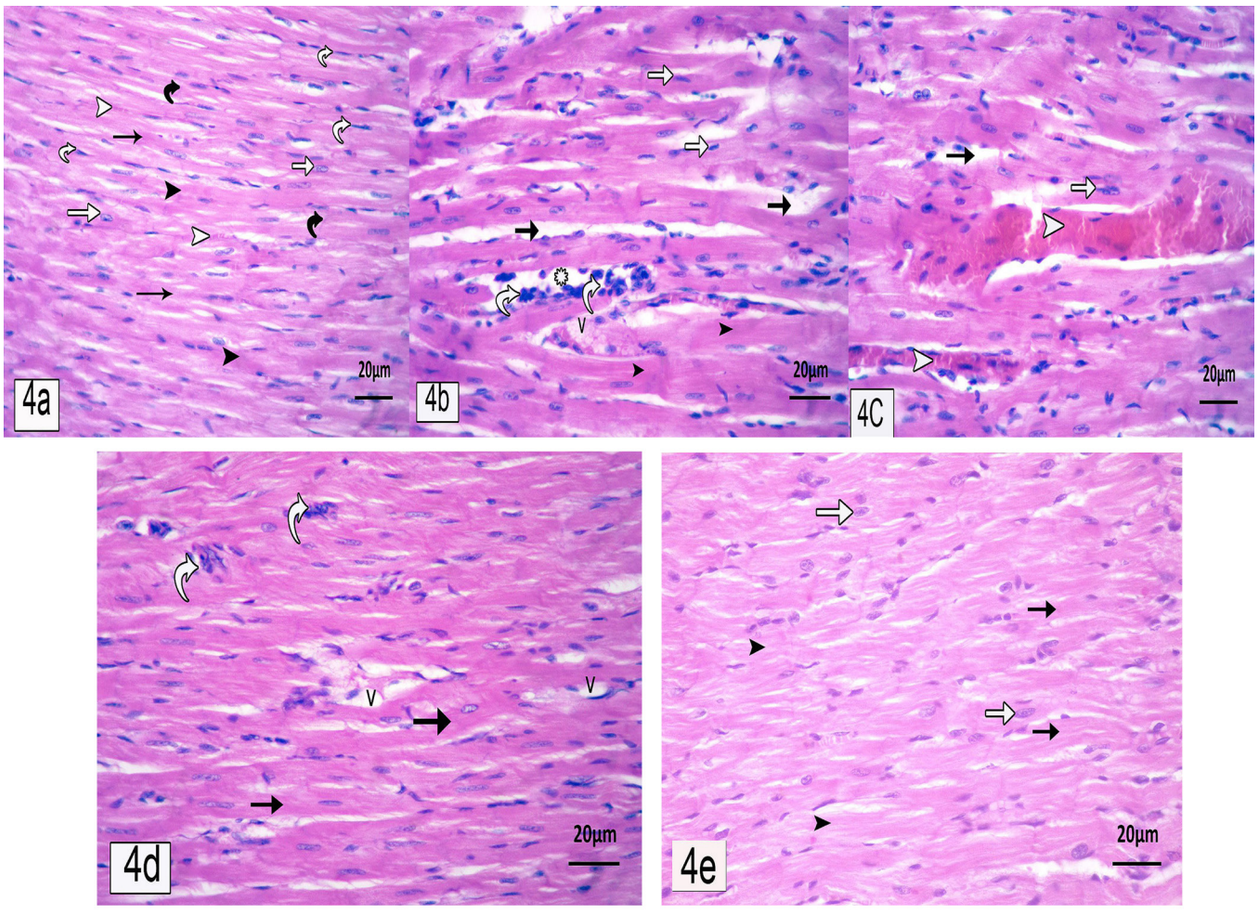

Figure 4: A Photomicrographs of H&E-stained myocardial sections of: (4a) Control group showing regular branching and reconnecting cardiac muscle cells (arrow). The cardiac myocytes appear with eosinophilic cytoplasm (arrowhead) and centrally located oval vesicular nuclei (white arrow). Intercalated discs appear as transverse dark lines (curved arrow). Few small blood capillaries (white arrowhead) and connective tissue cells nuclei (curved white arrow) are also shown in the intercellular endomysium spaces. (4b, 4c) Diabetes group showing fragmentation, and separation of cardiac muscle cells (arrow). Focal hypereosinophilia (arrowhead), cytoplasmic vacuolization (v), and peripheral dark nuclei (white arrow) can also be noticed. Inflammatory cellular infiltration (curved white arrow) and dilated (white arrowhead) or extravasated blood (RBCs) are seen. (4d) MSCs-treated group showing mildly preserved cardiomyocyte (arrow) and minimal vacuolization (v) of the cytoplasm. Few cellular infiltrations are still shown (curved white arrow). (4e) MLT–preconditioned MSCs group showing an apparently normal histological picture of branched and anastomosed cardiac muscle cells (arrow). The cardiac myocytes have eosinophilic cytoplasm (arrowhead) and centrally located oval vesicular nuclei (white arrow). (a, b, c, d, e X400, scale bar = 20 µm).

Table 3: Mean ± SD of area % of collagen fibers, optical density of TNF-α and Casp-3 proteins immune expressions and mean count quantity of homed fluorescent tagged MCs in left ventricle specimens of the studied groups:

	Group I	Group II	Group III	Group IV
Area % of collagen fibers	1.04 ± 0.48	3.4 ± 2.36#	2.8 ± 0.05*#	1.15 ± 0.08*&
Optical density of TNF-α protein immune expression	1.5 ± 0.35	9.3 ± 1.7#	3.81± 1.61*#	1.7 ± 0.25*&
Optical density of casp-3 protein immune expression	2.13 ± 0.7	10.82 ± 1.01#	3.81± 1.02*#	2.15 ± 0.6*&
Quantity of homed fluorescent tagged MCs	-	-	20 ± 1.8	39 ± 1.6&

 # P < 0.05 as related to group I
** P < 0.05 as related to group II*
& P < 0.05 as related to group III

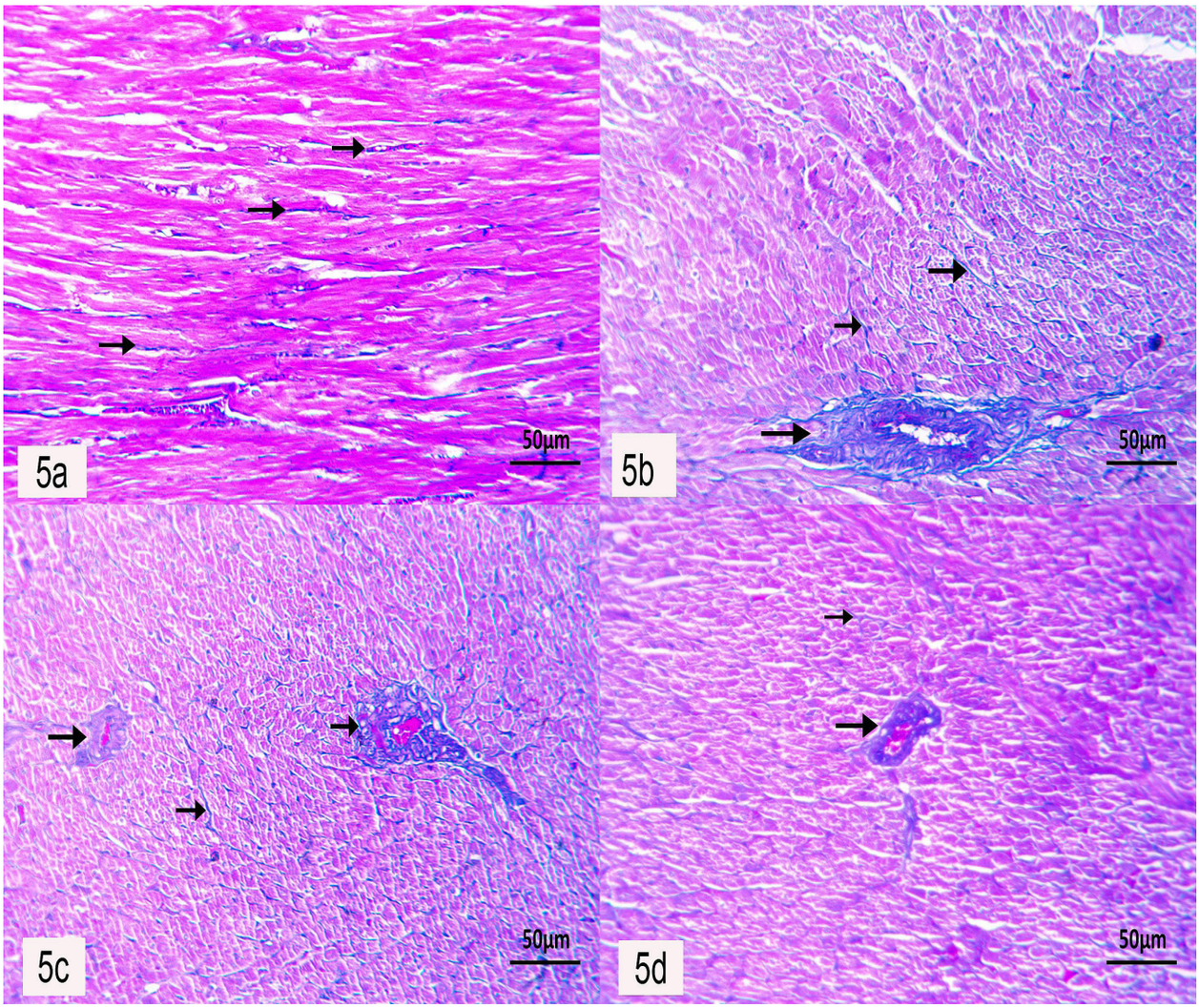

Figure 5: Masson's trichrome stained myocardial sections of: (5a) Control group showing fine blue collagen fibers in between the cardiac muscle cells and nearby small blood vessels (arrow). (5b) Diabetes group showing extensive collagen fibers deposition around dilated large blood vessel (arrow). (5c) MSCs-treated group showing moderate collagen fiber deposition (arrow). (5d) MLT–preconditioned MSCs group showing few collagen fibers around a blood vessel (arrow). (a, b, c, d X200, scale bar = 50 µm).

3.7.3. Immunohistochemical results:

Regarding anti-TNFα antibody immunohistochemical-stained sections; control group showed negative immune reaction of cardiac muscle cells and interstitial cells (Figure 6a). Markedly positive cytoplasmic immune reaction in the form of brown coloration of cardiac muscle cells and interstitial cells was noticed in the diabetic group (Figure 6b). MSCs-treated group revealed moderate positive immune reaction in the cardiomyocyte and the interstitial cells nuclei (Figure 6c). MLT–preconditioned MSCs group showed minimal positive immune reaction in cardiac muscle cells and interstitial cells (Figure 6d). The anti-casp-3 antibody immunohistochemical-stained sections of the control group and MLT–preconditioned MSCs group showed negative immune staining in the cardiac muscle fibers and interstitial cells (Figure 6e, 6h). Marked positive casp-3 immune reaction was noticed in the diabetic group in the form of brown coloration of the sarcoplasm, nuclei of heart muscle cells and interstitial cells (Figure 6f). MSCs-treated group displayed mild positive immune reaction in the sarcoplasm, some nuclei of cardiac muscle fibers and interstitial cells (Figure 6g).

3.7.4. Ultrastructural results:

Ultrathin sections of the control group showed longitudinally arranged cardiomyocyte with oval central euchromatic nuclei and prominent nucleoli. Long parallel intracytoplasmic myofibrils with the

sarcomere's unique structural pattern of alternating dark (A) bands with their central pale (H) zones and central (M) lines and light (I) bands which divided by (Z) lines were shown (Figure 7a). Multiple lines of variable sized mitochondria were placed among myofibrils and in the perinuclear space were seen. T-tubules were demonstrated at (Z) lines levels (Figure 7b). Intact intercalated discs with step-like characteristic pattern were also seen (Figure 7c). Cardiomyocytes from diabetic group showed irregular nuclear outline and aggregates of heterochromatin. Additionally, perinuclear vacuolization was seen. Myofibrils showed fragmentation, focal lysis of the myofilaments, vacuolization of the sarcoplasm and many discontinued (Z) lines. Moreover, ruptured irregularly arranged mitochondria with disrupted membranes and cristae were found. Accumulation of interstitial collagen fibers was observed. (Figure 7d, 7e). Non continuous dilated intercalated discs with areas devoid of junctions were seen. (Figure 7f). In MSCs-treated group cardiomyocytes expressed mild changes in the form of focal areas of degenerated and fragmented myofilaments with loss of sarcomeres pattern. Some distorted mitochondria with disrupted membrane and cristae were seen in between myofibrils (Figure 8a). Dark shrunk nucleus was demonstrated (Figure 8b). While in MLT–preconditioned MSCs group, cardiomyocytes apparently preserved the normal histological features in the form of intact myofibrils with the normal sarcomeres pattern (Figure 8c). The mitochondria appeared normal and settled in lines among myofibrils in the perinuclear region. The nuclei appeared oval with extended chromatin and prominent nucleoli. (Figure 8d).

3.8. Real-time (qRT-PCR) relative mRNA expression:

A significant increase of Bcl-2 and IL-10 genes expression in MSCs-treated groups when compared to the diabetic group was revealed. MLT-preconditioned MSCs group showed significant upregulation of antiapoptotic Bcl-2 and anti-inflammatory IL-10 mRNA expression as compared to the MSCs-treated group ($P < 0.001$, $P < 0.001$, $P = 0.05$, subsequently). Moreover, there was a significant down-regulation of proapoptotic marker casp-3 and the pro-inflammatory marker IL-1β in MSCs-treated rat groups as compared to the diabetic rats. MLT-preconditioned MSCs group expressed significant downregulation of mRNA expression of casp-3 and IL-1β compared to the MSCs-treated rat group (Table 4).

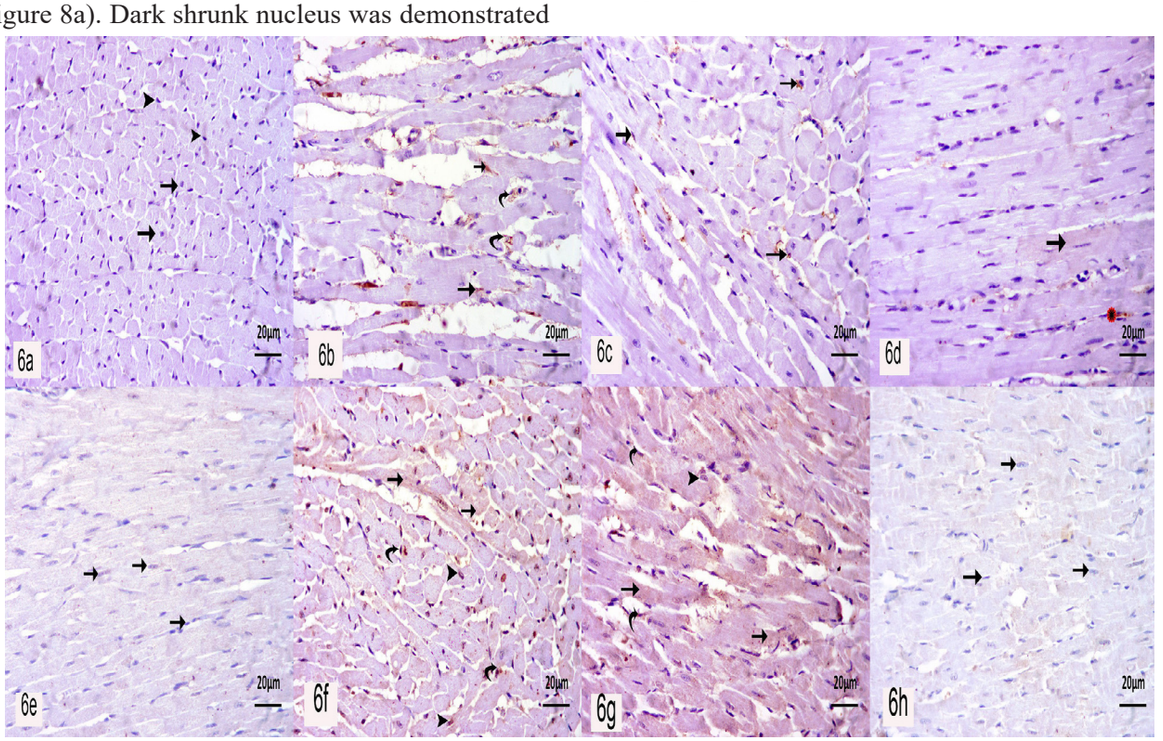

Figure 6: Photomicrograph of a sections in myocardium of: (6a) Control group showing negative immune reaction of TNFα in the cardiac muscle cells (arrow)and interstitial cells (arrowhead), (6b) Diabetic group showing markedly positive cytoplasmic immune reaction of TNFα in cardiac muscle cells (arrow) and interstitial cells (curved arrow), (6c) MSCs-treated group showing moderately positive immune reaction of TNFα in the interstitial cells nuclei (arrow), (6d) MLT-predisposed MSCs group shows minimal positive immune reaction in cardiac muscle cells (arrow) and interstitial cells (*) (Anti-TNFα, immunostaining, a, b, c, d X400, scale bar 20 µm). (6e) control and (6h) MLT–preconditioned MSC groups showing negative immune reaction of Casp-3 in cardiac muscle cells, and interstitial cells (arrow), (6f) Diabetic group showing marked positive immune reaction of Casp-3 in form of brown coloration in sarcoplasm (arrow) and nuclei of cardiac muscle cells (arrowhead) and interstitial cells (curved arrow) nuclei, (6g) MSC group showing mild positive immune reaction of Casp-3 in sarcoplasm (arrow), nuclei of cardiac muscle cells (arrowhead) and interstitial cells nuclei (curved arrow). (Anti Casp-3 immunostaining, e, f, g, h X400, scale bar 20 µm)

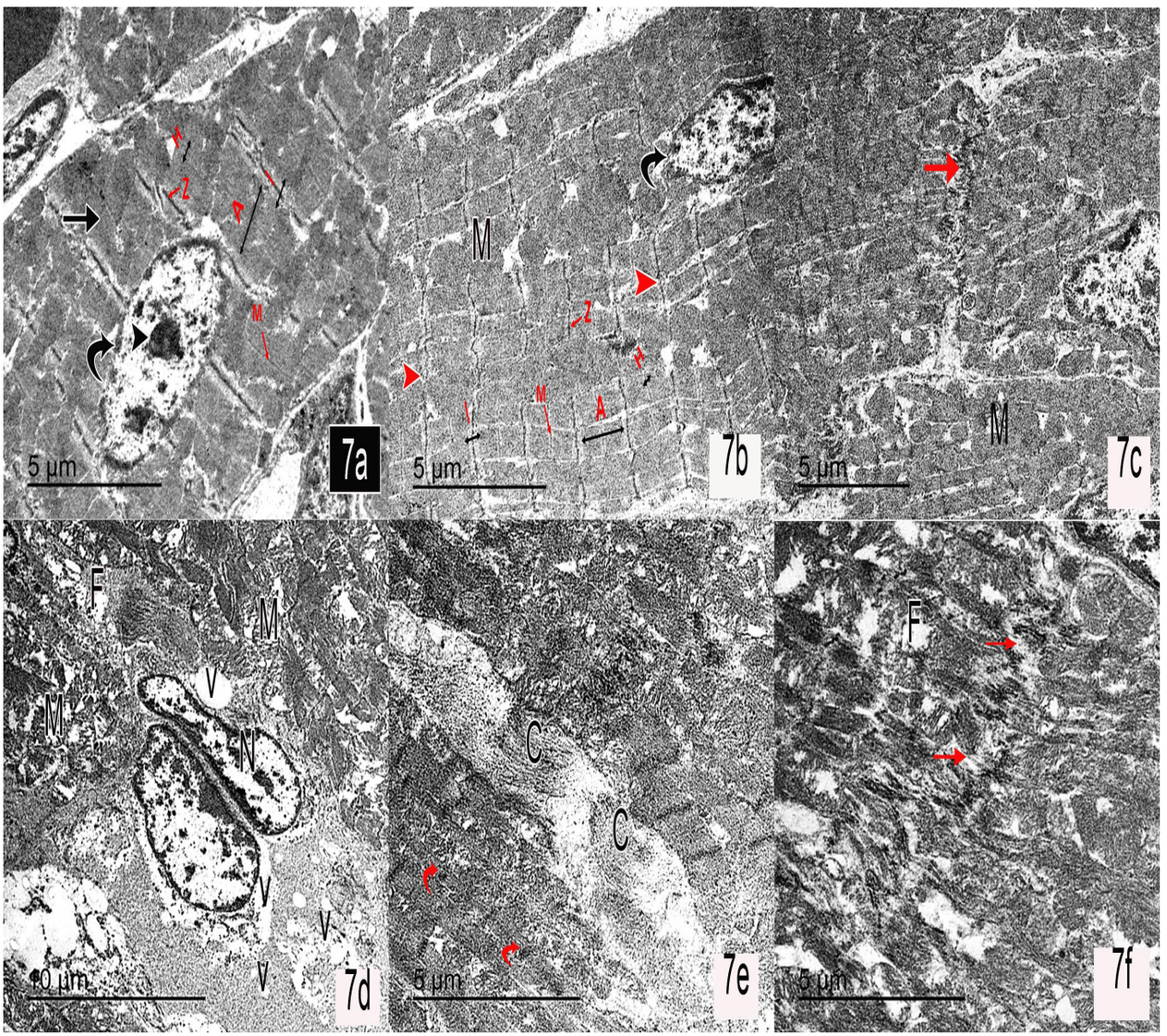

Figure 7: Pho An electron micrograph of ultrathin section in the cardiomyocytes of: Control group (7a-7c) showing (7a) a longitudinally arranged cardio myocyte (arrow) with central oval euchromatic nuclei (curved arrow) and prominent nucleoli (arrowhead). Long parallel myofibrils with the sarcomere's structural pattern of alternating dark [A] bands with their central pale [H] zones and central [M] lines and light [I] bands which is divided by [Z] lines are also shown. (7b) Multiple lines of variable sized mitochondria (M) are placed among myofibrils and in the perinuclear zone. T tubules (red arrow head) are demonstrated at the level of (Z) lines. (7c) Intact intercalated discs with step-like characteristic pattern are noticed (red arrow). Diabetic group (7d, 7e) showing distorted nuclei with irregular outline and aggregates of heterochromatin (N). Perinuclear vacuolization (V) is noticed. Myofibrils showing fragmentation, focal lysis (F), vacuolization of the sarcoplasm (V) and many discontinued (Z) lines (red curved arrow). Many ruptured irregularly arranged mitochondria with disrupted membranes and cristae are noticed (M). Massive accumulation of interstitial collagen fibers (C) is seen. (7f) Non continuous dilated intercalated discs with areas devoid of junctions are seen (red arrow). (a, b, c, d, e, f X 1200 Scale bar =5µm).

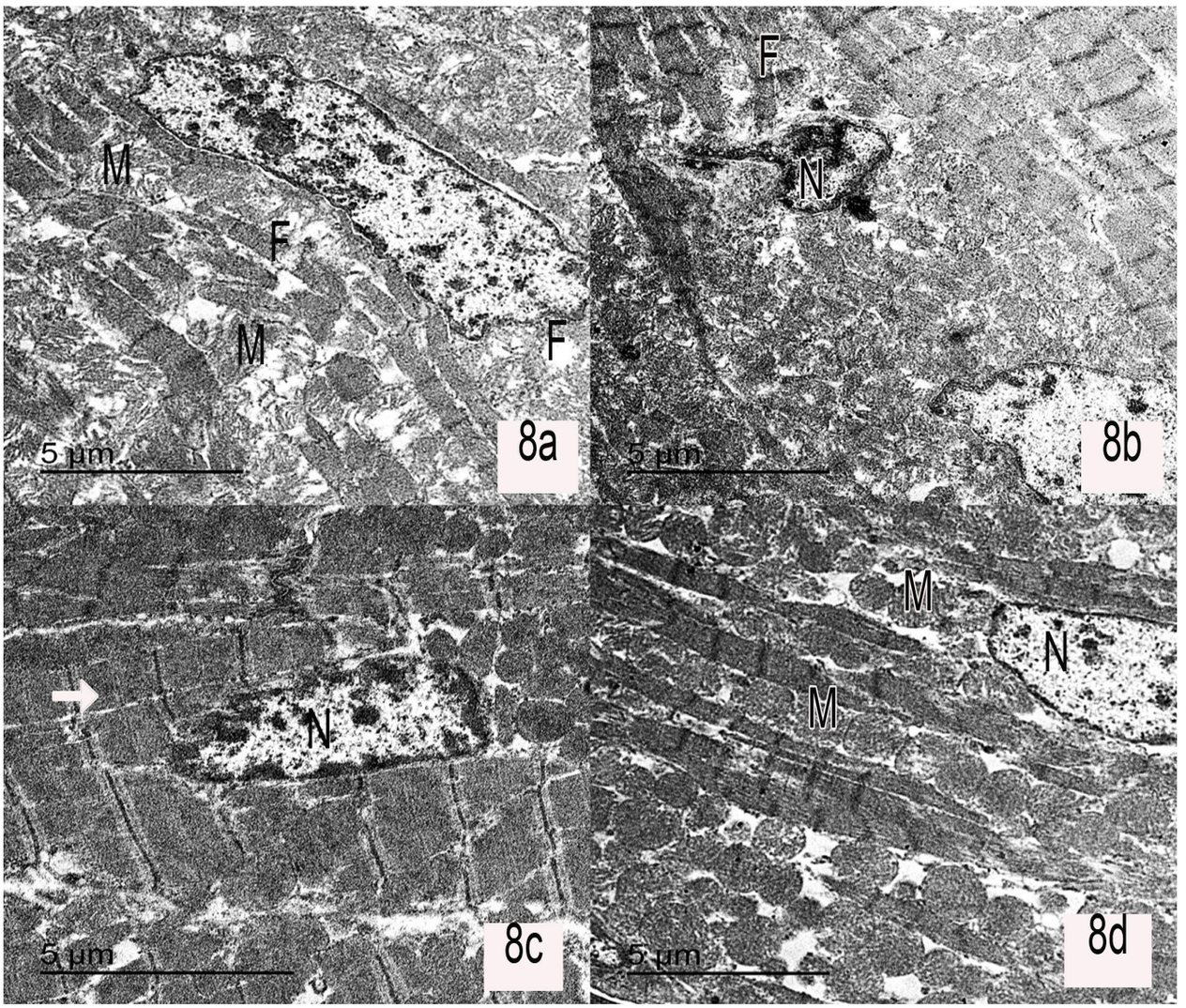

Figure 8: An electron micrograph of ultrathin section in the cardiomyocytes of: MSCs-treated group (8a, 8b) showing: (8a) focal areas of degenerated and fragmented myofilaments (F) with loss of sarcomeres pattern. Some distorted mitochondria with disrupted membrane and cristae (M) are shown in between myofibrils. (8b) darkly stained shrunken nucleus (N) is noticed. MLT–preconditioned MSC group (8c, 8d) showing: (8c) apparently preserved normal histological features in the form of intact myofibrils with the normal sarcomeres pattern (arrow). (8d) The mitochondria (M) are normal and placed in rows among myofibrils and deposited in the perinuclear region. The nuclei are oval with extended chromatin and prominent nucleoli (N). (a, b, c, d X 1200 Scale bar = 5µm).

3.9. Histo-morphometric results:

The concluded statistical findings for the area percentage of collagen fibers, optical density of TNF-α and Casp-3 proteins immune expression and mean count of homed fluorescent tagged MSCs in left ventricle sections of the studied rat groups are summarized in (Table 4). There was a significant increase in area percentage of collagen fibers content in myocardium of diabetic rats (group II) (3.4 ± 2.36) compared to control group (1.04 ± 0.48) ($P < 0.05$) while a significant decrease in its expression in group III and IV (2.8 ± 0.05 and 1.15 ± 0.08, respectively) ($P < 0.05$). Meanwhile, the decrease in the area percentage of collagen fiber in group IV was of a statistical significance compared to group III ($P < 0.05$) and of non-statistically significant difference when compared to group III ($P > 0.05$).

The optical density of TNF-α in the immunohistochemical stained cardiac section of group II displayed a significant increase (9.3 ± 1.7) compared to the control group (1.5 ± 0.35) ($P < 0.05$) while a significant decrease was noted in group III and IV (3.81 ± 1.61 and 1.7 ± 0.25, respectively) ($P < 0.05$). The optical density of Casp-3 expression in myocardium of group II also displayed a significant increase (10.82 ± 1.01) compared to the control group (2.13 ± 0.7) ($P < 0.05$) while

its expression in myocardium of group III and IV (3.81 ± 1.02 and 2.15 ± 0.6, respectively) was decreased and found to be very near to the control values in group IV. The decrease in the optical density of TNF-α and Casp-3 in group IV was of a statistical significance compared to group III ($P < 0.05$) and of non-statistically significant difference when compared to group III ($P > 0.05$).

Table 4: Findings of real-time (qRT-PCR) relative to mRNA expression in the heart tissue of all the examined groups:

	Group I	Group II	Group III	Group IV
Bcl 2	1 ± 0.02	1.25 ± 0.03#	1.5 ± 0.01#*	1.6 ± 0.02#*&
Casp 3	1 ± 0.01	0.79 ± 0.01#	0.69 ± 0.02#*	0.44 ± 0.03#*&
IL-10	1 ± 0.01	1.13 ± 0.04#	1.51 ± 0.03#*	1.85 ± 0.02#*&
IL-1β	1 ± 0.01	0.89 ± 0.01#	0.84 ± 0.02#*	0.76 ± 0.02#*&

 # P < 0.05 as related to group I
** P < 0.05 as related to group II*
& P < 0.05 as related to group III

DISCUSSION

Cardiomyopathy is an evident impediment of diabetes mellitus (de Ferranti *et al.* 2014) Many researchers have illustrated that DC are associated with apoptotic changes, these changes are accounted for subsequent possible fibrosis, hypertrophy, and cardiac dysfunction (Zhang *et al.* 2016). In the current study, many altered cardiac histopathological and ultrastructural picture in the DC rat experimental model in the form of degeneration, fragmentation with focal loss of the sarcoplasm. Irregular nuclei with aggregation of heterochromatin and perinuclear vacuolization. Discontinuous Z lines and area devoid of cell junction inside the intercalated discs. Such alterations could be explained by reactive oxygen species (ROS) generation. It is the direct cause for lipid peroxidation, facilitate DNA damage, destruction of lipid and protein cellular components, and finally stromal cell damage and concomitant cell apoptosis (Mustafa *et al.* 2017; Ni *et al.* 2020).

Increased blood glucose level in diabetes mellitus was also proved to foster the synthesis of (ROS) that in turn could enhance cell death via cytochrome-c-mediated caspase-3 activation, and subsequently affects the expansion and endurance of multipotent stem cells and precursor cells residing the heart (Yang *et al*. 2017). As found in this work, other studies revealed that transplantation of BM-MCs was recorded to decrease Casp-3 expression in the myocardium of DCM rat model, improve the histopathological picture of the heart and reduce cardiac apoptosis by decreasing Bax /Bcl2 ratio (Dong *et al.* 2014).

Our findings denoting many ruptured irregularly arranged mitochondria in the diabetic group. Mitochondrial membranes are the target sites for lipid peroxidation that affects its stability and permeability with subsequent inhibition of its enzymatic activity and ATP generation which directly lead to cell death (Lai *et al.* 2011). Also, we noticed many cytoplasmic vacuolization, similar findings were explained by a widening of sarcoplasmic reticulum and T tubules due to its membrane hydropic degeneration (Chugun *et al*. 2000). In the same group, an inflammatory cellular infiltration and dilated congested blood vessels were found. This could be a sequence of inflammatory cascade that accompanying DC and this was supported by upregulation of pro-inflammatory mediators IL-1β gene expression in the cardiac tissue which was estimated in the same group. Chronic hyperglycemia was also claimed to increase advanced glycation endproduct (AGE) in cardiac extracellular matrix and enhance the detention of pro-inflammatory markers, counting TNF-α, IL-6, Intercellular Adhesion Molecule 1 (ICAM-1), and CC motif chemokine ligand 2 (Wenzl *et al.* 2021). Transplantation of human umbilical HU-MSCs was able to reduce TNF α expression when transplanted into a rat model of DCM (Mao *et al.* 2017; Zhang *et al.* 2017).

The current study declared that the administration of MLT-predisposed MSCs causes a significant upregulation of IL-10 and downregulation of IL-1β expression. IL-10 is a prime multi action immunomodulatory markers that avert destruction of host cells through exerting immunosuppressive effects. This action is expressed through the enhancement of B cells multiplication and the elevation of B-reg cells number (Gupte *et al.* 2017).

Similarly, Meng *et al.* reported that IL-10-transfected MSCs showed increased IL-10 secretion promoting cell viability and decreasing the resultant myocardia inflammatory reaction, injury, and apoptosis in rats with myocardial infarction (MI) (Meng *et al.* 2018). Meanwhile Sheu *et al.* (2021) noted that the inhibitory effect of IL-1β secretion by human-induced iPSC -MSCs was competent to abolish the inflammatory reaction and boost the restoration of cardiac performance in rats with dilated cardiomyopathy through miR-19a and miR-20a overexpression (Sheu *et al.* 2021).

It is known that SCs have a cardiac reparative property either by transformation into cardiomyocytes, vascular endothelial cells and smooth muscle cells of blood vessels

(Orlic *et al*. 2001) or mainly by their secretome, which decrease inflammatory reactions and enhance new vessels formation, ensuring cardiac tissue guarding (Quevedo *et al*. 2009).

Our results showed that transplantation of both non predisposed and predisposed BM-MSCs significantly improved the ultrastructure of the rat heart. In several research, many stem cell types have been consistent with lessen remodeling to reestablish destructed cardiomyocytes and enhancing cardiac performance (Boheler *et al*. 2005; Kanamori *et al*. 2015; Selem, Hatzistergos, and Hare 2013). Among those types BM-MSCs were widely used and act by enhancement of cardiomyocytes regeneration, expression trans differentiation and cells fusion (Wu *et al*. 2015).

This study revealed that collagen deposition and heart fibrosis increased significantly in diabetic rats of group II. The same finding was recorded in many previous studies and explained by upregulation of both type I and type III collagen, in addition to, increase in connective tissue growth factor (CTGF) in myocardium of DCM rat model (Kania, Blyszczuk, and Eriksson 2009; Zhang *et al*. 2017). Many studies have found that fibroblasts could migrated to the site of tissue injury and proliferated into myofibroblasts, that lay down large amount of collagen fibers leading to obvious fibrosis and may leads to heart failure. It was also found that transplantation of MSCs and MLT-predisposed MSCs to diabetic rats of group III and IV, respectively, decreased the collagen content and increased cardiac muscle fibers content (Tarbit *et al*. 2019). Zhang *et al*., stated that (HuMSCs) boost cardiac behavior by reducing myocardial reorganization of collagen network through decreasing TGF-β1 and TNF-α mRNA expression and acceleration of extracellular-signal-regulated kinase (ERK12/) communicating in DCM rats (Zhang *et al*. 2017). The same results were recorded by instillation of adipose derived MSCs in DCM rats and the underlying mechanism was stated to be the function of prostaglandine-2 (PGE2) secreted by MSCs. Moreover, MSCs also have an anti-collagen deposition effect, minimizing heart fibroblast function and fibrosis, and they indorse innermost reconstruction by provocation heart resident SCs and heart progenitor cells (Jin *et al*. 2020).

Our findings disclosed a significant increase of TNF-α and Casp-3 in immunohistochemical stained myocardium of the diabetic nontreated rats. TNF-α is a proinflammatory mediator with a broad spectrum of biological properties, it is essentially produced by triggered macrophages, T lymphocytes, and natural killer (NK) cells (Jin *et al*. 2020). It was proved to be elaborated in the pathophysiology of many cardiovascular insults. Its overproduction causes adverse cardiac remodeling through increasing amount of matrix metalloproteinase (MMP) action and increased collagen deposition (Aronson. Jeffrey K 2016). The expression of TNF-α was decreased significantly in the rat's myocardium of the MLT-MCs treated group in our study. This was in an accordance with Westermann *et al*., who proved that Inhibition of TNF α reduced the incidence of myocardial inflammatory process and collagen deposition through reduced (ERK) phosphorylation diabetic cardiomyopathy in experimental animals (Westermann *et al*. 2007).

The current study declared a significant upregulation of Bcl-2 and downregulation of Casp-3 expression after the administration of MLT-predisposed MSCs both in vivo and in vitro which could be explained based on the paracrine properties of MSCs that boost survival and proliferation of myocardial cells, rationalizing the cardiac profit owed by stem cell, notably the Bcl-2 -overexpressing MSCs. Bcl-2 is a salient preventer of ventricular cardiomyocytes cell death, while Bax is a pro-apoptotic protein (Li *et al*., 2007). Multiple studies had proved the protective effects of Bcl-2 on the failing hearts through its role as a metabolic regulator of mitochondrial functions during hypoxic conditions (Imahashi *et al*. 2004; Kirshenbaum and de Moissac 1997). In parallel, Li *et al*., demonstrated that Bcl-2 adjusted MSCs transplantation overexpressed vascular endothelial growth factor (VEGF) in response to hypoxia which substantially improved left ventricular (LV) remodeling and LV function (Li *et al*. 2007).

Cell death can be provoked by two communication pathways: the outer (death receptor) and the inner (mitochondria-mediated) pathways. Both outer and inner cell death signaling motivates the stimulation of casp-3 (the final executive effector of apoptosis), which in turn activates numerous subsequent caspases (casp-6 and casp-7) amplify the death signal, cleave the vital structural proteins including myofibrillar proteins and induce apoptosis in cardiomyocytes resulting in contractile dysfunction (Yang, Ye, and Wang 2013).

Caspases, in addition to forcing apoptosis, cause under expression of serine/threonine protein kinase Akt (Akt) in that is proved to enhance cell endurance (Saini *et al*. 2013).

In the same token, Mohamed *et al* declared that MSC-mediated inhibition of Casp-3 expression can reduce cardiomyocyte apoptosis and consequently ameliorate cardiac function (Mohamed *et al*. 2015).

In the current research tracking of the transplanted cells revealed that PKH-26 labelled BM-MSCs were detected in the rat heart sections after 4 weeks of transplantation in the recipient groups of MLT-predisposed and non-predisposed MSCs with better recruitment affinity and survivability of the MLT-predisposed SCs.

Modalities of SCs therapy were studied in various research to improve their cardiac reparative power including predisposing by different substances or their epigenetic modification. Our results revealed that MLT-predisposed MSCs efficacy in cardiac tissue preservation was recorded to be increased significantly compared to the non-predisposed MSCs. Similarly, improvement in stem cell persistence, therapeutic possibility and cardioprotective was explored after intravenous intake of BM-MSCs bind with resveratrol (an antioxidant) in diabetic rats (Gallina, Turinetto, and Giachino 2015). Moreover, MLT- predisposed SCs showed a significant enhancement of their survivability and their engraftment in many different diseased tissues (Delucchi *et al*. 2012; Mortezaee *et al*. 2016; Saberi *et al*. 2019; Zhao *et al*. 2020).

CONCLUSION

BM- MSCs and MLT-Preconditioned-BM-MSCs are a highly encouraging restorative policy for the treatment of DCM acting by attenuating cardiac remodeling, decreasing cardiac fibrosis, cardiomyocyte apoptosis which proved by both histopathological and immunohistochemical methods. downregulating inflammatory cytokines (IL-1β) and apoptotic marker (Casp-3) within the cardiomyocytes. They were also proved to upregulate the mRNA expression of the antiapoptotic gene Bcl-2 and the anti-inflammatory IL-10 within the same tissue. Preconditioning of BM-MSCs with Melatonin (1 μm) significantly improved their efficacy compared to the non-preconditioned BM-MSCs by increasing their survivability and recruitment in the tissue hence, enhancing their antiapoptotic and immunomodulatory activities. So, preconditioning of BM-MSCs with MLT may be considered an appropriate avenue for elaborating the valuable outcomes of MSCs regimen in DCM, However, further research is recommended for appropriate assessment of the cardiac function and the long-term consequence of this type of cytotherapy. In our

CONFLICT OF INTEREST

There is no potential conflict of interest among the authors.

REFERENCES

1. Abas, Eman, and Marwa Sabry. 2020. “Intermittent Fasting Attenuates Apoptosis, Modulates Autophagy and Preserve Telocytes in Doxorubicin Induced Cardiotoxicity in Albino Rats: A Histological Study.” Egyptian Journal of Histology.

2. Abd El-kader, Marwa. 2019. “Evaluation of Azithromycin Induced Cardiotoxicity in Male Albino Rats and the Possible Protective Role of Nigella Sativa Oil.” Egyptian Journal of Histology.

3. Abdollahi, M., A. B. Z. Zuki, Y. M. Goh, A. Rezaeizadeh, and M. M. Noordin. 2011. “Effects of Momordica Charantia on Pancreatic Histopathological Changes Associated with Streptozotocin-Induced Diabetes in Neonatal Rats.” Histology and Histopathology 26(1):13–21.

4. Annadurai, T., A. R. Muralidharan, T. Joseph, M. J. Hsu, P. A. Thomas, and P. Geraldine. 2012. “Antihyperglycemic and Antioxidant Effects of a Flavanone, Naringenin, in Streptozotocin-Nicotinamide-Induced Experimental Diabetic Rats.” Journal of Physiology and Biochemistry 68(3):307–18.

5. Aronson. Jeffrey K. 2016.Pp. 230–32 in Meyler’s Side Effects of Drugs: The International Encyclopedia of Adverse Drug Reactions and Interactions. Vol. seven, volume 7. Elsevier.

6. Bancroft J., Gamble, M. 2013.Pp. 165–75 in Theory and Practice of Histological Techniques. Churchill Livingston, New York, Edinburgh, London.

7. Boheler, Kenneth R., David G. Crider, Yelena Tarasova, and Victor A. Maltsev. 2005. “Cardiomyocytes Derived from Embryonic Stem Cells.” Methods in Molecular Medicine 108:417–35.

8. Chen, Weikai, Nanning Lv, Hao Liu, Chao Gu, Xinfeng Zhou, Wanjin Qin, Angela Carley Chen, Liang Chen, Huilin Yang, Xi Chen, Tao Liu, and Fan He. 2022. “Melatonin Improves the Resistance of Oxidative Stress-Induced Cellular Senescence in Osteoporotic Bone Marrow Mesenchymal Stem Cells” edited by T. Maraldi. Oxidative Medicine and Cellular Longevity 2022:1–22.

9. Chen, Ying, Qiuhao Yu, and Cang-Bao Xu. 2017. “A Convenient Method for Quantifying Collagen Fibers in Atherosclerotic Lesions by ImageJ Software”.

10. Chugun, A., K. Temma, T. Oyamada, N. Suzuki, Y. Kamiya, Y. Hara, T. Sasaki, H. Kondo, and T. Akera. 2000. "Doxorubicin-Induced Late Cardiotoxicity: Delayed Impairment of Ca2+-Handling Mechanisms in the Sarcoplasmic Reticulum in the Rat." Canadian Journal of Physiology and Pharmacology 78(4):329–38.

11. Cooney, Damon S., Eric G. Wimmers, Zuhaib Ibrahim, Johanna Grahammer, Joani M. Christensen, Gabriel A. Brat, Lehao W. Wu, Karim A. Sarhane, Joseph Lopez, Christoph Wallner, Georg J. Furtmüller, Nance Yuan, John Pang, Kakali Sarkar, W. P. Andrew Lee, and Gerald Brandacher. 2016. "Mesenchymal Stem Cells Enhance Nerve Regeneration in a Rat Sciatic Nerve Repair and Hindlimb Transplant Model." Scientific Reports 6(1):31306.

12. Delucchi, Francesca, Roberta Berni, Caterina Frati, Stefano Cavalli, Gallia Graiani, Roberto Sala, Christine Chaponnier, Giulio Gabbiani, Luca Calani, Daniele Del Rio, Leonardo Bocchi, Costanza Lagrasta, Federico Quaini, and Donatella Stilli. 2012. "Resveratrol Treatment Reduces Cardiac Progenitor Cell Dysfunction and Prevents Morpho-Functional Ventricular Remodeling in Type-1 Diabetic Rats." PloS One 7(6):e39836.

13. Dominici, M., K. Le Blanc, I. Mueller, I. Slaper-Cortenbach, Fc Marini, Ds Krause, Rj Deans, A. Keating, Dj Prockop, and Em Horwitz. 2006. "Minimal Criteria for Defining Multipotent Mesenchymal Stromal Cells. The International Society for Cellular Therapy Position Statement." Cytotherapy 8(4):315–17.

14. Dong, Xiaoyan, Fen Zhu, Qun Liu, Yuanheng Zhang, Jun Wu, Wen Jiang, Lei Zhang, and Shuguang Dong. 2014. "Transplanted Bone Marrow Mesenchymal Stem Cells Protects Myocardium by Regulating 143-3- Protein in a Rat Model of Diabetic Cardiomyopathy." International Journal of Clinical and Experimental Pathology 7(7):3714–23.

15. El-Akabawy, Gehan, and Wael El-Kholy. 2014. "Neuroprotective Effect of Ginger in the Brain of Streptozotocin-Induced Diabetic Rats." Annals of Anatomy = Anatomischer Anzeiger: Official Organ of the Anatomische Gesellschaft 196(2–3):119–28.

16. Emsley, Richard, Graham Dunn, and Ian R. White. 2010. "Mediation and Moderation of Treatment Effects in Randomised Controlled Trials of Complex Interventions." Statistical Methods in Medical Research 19(3):237–70.

17. Fang, Jia, Yuan Yan, Xin Teng, Xinyu Wen, Na Li, Sha Peng, Wenshuai Liu, F. Xavier Donadeu, Shanting Zhao, and Jinlian Hua. 2018. "Melatonin Prevents Senescence of Canine Adipose-Derived Mesenchymal Stem Cells through Activating NRF2 and Inhibiting ER Stress." Aging 10(10):2954–72.

18. de Ferranti, Sarah D., Ian H. de Boer, Vivian Fonseca, Caroline S. Fox, Sherita Hill Golden, Carl J. Lavie, Sheela N. Magge, Nikolaus Marx, Darren K. McGuire, Trevor J. Orchard, Bernard Zinman, and Robert H. Eckel. 2014a. "Type 1 Diabetes Mellitus and Cardiovascular Disease: A Scientific Statement from the American Heart Association and American Diabetes Association." Diabetes Care 37(10):2843–63.

19. de Ferranti, Sarah D., Ian H. de Boer, Vivian Fonseca, Caroline S. Fox, Sherita Hill Golden, Carl J. Lavie, Sheela N. Magge, Nikolaus Marx, Darren K. McGuire, Trevor J. Orchard, Bernard Zinman, and Robert H. Eckel. 2014b. "Type 1 Diabetes Mellitus and Cardiovascular Disease: A Scientific Statement from the American Heart Association and American Diabetes Association." Diabetes Care 37(10):2843–63.

20. Gallina, Clara, Valentina Turinetto, and Claudia Giachino. 2015. "A New Paradigm in Cardiac Regeneration: The Mesenchymal Stem Cell Secretome." Stem Cells International 2015:765846.

21. Gupte, Kunal S., Aruna V. Vanikar, Hargovind L. Trivedi, Chetan N. Patel, and Jignesh V. Patel. 2017. "In-Vitro Generation of Interleukin-10 Secreting B-Regulatory Cells from Donor Adipose Tissue Derived Mesenchymal Stem Cells and Recipient Peripheral Blood Mononuclear Cells for Potential Cell Therapy." Biomedical Journal 40(1):49–54.

22. Haas, Stefan Jean Pierre, Peter Bauer, Arndt Rolfs, and Andreas Wree. 2000. "Immunocytochemical Characterization of in Vitro PKH26-Labelled and Intracerebrally Transplanted Neonatal Cells." Acta Histochemica 102(3):273–80.

23. Hare, Joshua M., Darcy L. DiFede, Angela C. Rieger, Victoria Florea, Ana M. Landin, Jill El-Khorazaty, Aisha Khan, Muzammil Mushtaq, Maureen H. Lowery, John J. Byrnes, Robert C. Hendel, Mauricio G. Cohen, Carlos E. Alfonso, Krystalenia Valasaki, Marietsy V. Pujol, Samuel Golpanian, Eduard Ghersin, Joel E. Fishman, Pradip Pattany, Samirah A. Gomes, Cindy Delgado, Roberto Miki, Fouad Abuzeid, Mayra Vidro-Casiano, Courtney Premer, Audrey Medina, Valeria Porras, Konstantinos E. Hatzistergos, Erica Anderson,

Adam Mendizabal, Raul Mitrani, and Alan W. Heldman. 2017. "Randomized Comparison of Allogeneic Versus Autologous Mesenchymal Stem Cells for Nonischemic Dilated Cardiomyopathy: POSEIDON-DCM Trial." Journal of the American College of Cardiology 69(5):526–37.

24. Houtgraaf, Jaco H., Wijnand K. den Dekker, Bas M. van Dalen, Tirza Springeling, Renate de Jong, Robert J. van Geuns, Marcel L. Geleijnse, Francisco Fernandez-Aviles, Felix Zijlsta, Patrick W. Serruys, and Henricus J. Duckers. 2012. "First Experience in Humans Using Adipose Tissue-Derived Regenerative Cells in the Treatment of Patients with ST-Segment Elevation Myocardial Infarction." Journal of the American College of Cardiology 59(5):539–40.

25. Imahashi, Kenichi, Michael D. Schneider, Charles Steenbergen, and Elizabeth Murphy. 2004. "Transgenic Expression of Bcl-2 Modulates Energy Metabolism, Prevents Cytosolic Acidification during Ischemia, and Reduces Ischemia/Reperfusion Injury." Circulation Research 95(7):734–41.

26. Jia, Yanhui, Zhao Zheng, Yunchuan Wang, Qin Zhou, Weixia Cai, Wenbin Jia, Longlong Yang, Maolong Dong, Xiongxiang Zhu, Linlin Su, and Dahai Hu. 2015. "SIRT1 Is a Regulator in High Glucose-Induced Inflammatory Response in RAW264.7 Cells." PloS One 10(3):e0120849.

27. Jin, Liyuan, Jinying Zhang, Zihui Deng, Jiejie Liu, Weidong Han, Guanghui Chen, Yiling Si, and Ping Ye. 2020. "Mesenchymal Stem Cells Ameliorate Myocardial Fibrosis in Diabetic Cardiomyopathy via the Secretion of Prostaglandin E2." Stem Cell Research & Therapy 11(1):122.

28. Kanamori, Hiromitsu, Genzou Takemura, Kazuko Goto, Akiko Tsujimoto, Atsushi Mikami, Atsushi Ogino, Takatomo Watanabe, Kentaro Morishita, Hideshi Okada, Masanori Kawasaki, Mitsuru Seishima, and Shinya Minatoguchi. 2015. "Autophagic Adaptations in Diabetic Cardiomyopathy Differ between Type 1 and Type 2 Diabetes." Autophagy 11(7):1146–60.

29. Kania, Gabriela, Przemyslaw Blyszczuk, and Urs Eriksson. 2009. "Mechanisms of Cardiac Fibrosis in Inflammatory Heart Disease." Trends in Cardiovascular Medicine 19(8):247–52.

30. Kirshenbaum, L. A., and D. de Moissac. 1997. "The Bcl-2 Gene Product Prevents Programmed Cell Death of Ventricular Myocytes." Circulation 96(5):1580–85.

31. Lai, Renchun, Yuhui Long, Qiuli Li, Xu Zhang4, and Tiehua Rong4. 2011. "Oxidative Stress Markers May Not Be Early Markers of Doxorubicin-Induced Cardiotoxicity in Rabbits." Experimental and Therapeutic Medicine 2(5):947–50.

32. Leask, Andrew. 2015. "Getting to the Heart of the Matter: New Insights into Cardiac Fibrosis." Circulation Research 116(7):1269–76.

33. Li, Balun, Xuedi Cheng, Aili Aierken, Jiaxin Du, Wenlai He, Mengfei Zhang, Ning Tan, Zheng Kou, Sha Peng, Wenwen Jia, Haiyang Tang, and Jinlian Hua. 2021. "Melatonin Promotes the Therapeutic Effect of Mesenchymal Stem Cells on Type 2 Diabetes Mellitus by Regulating TGF-β Pathway." Frontiers in Cell and Developmental Biology 9:722365.

34. Li, Tian, Shuai Jiang, Chenxi Lu, Wenwen Yang, Zhi Yang, Wei Hu, Zhenlong Xin, and Yang Yang. 2019. "Melatonin: Another Avenue for Treating Osteoporosis?" Journal of Pineal Research 66(2):e12548.

35. Li, Wenzhong, Nan Ma, Lee-Lee Ong, Catharina Nesselmann, Christian Klopsch, Yury Ladilov, Dario Furlani, Christoph Piechaczek, Jeannette M. Moebius, Karola Lützow, Andreas Lendlein, Christof Stamm, Ren-Ke Li, and Gustav Steinhoff. 2007. "Bcl-2 Engineered MSCs Inhibited Apoptosis and Improved Heart Function." Stem Cells (Dayton, Ohio) 25(8):2118–27.

36. Livak, Kenneth J., and Thomas D. Schmittgen. 2001. "Analysis of Relative Gene Expression Data Using Real-Time Quantitative PCR and the $2^{-\Delta\Delta CT}$ Method." Methods 25(4):402–8.

37. Mao, Chenggang, Xu Hou, Benzhen Wang, Jingwei Chi, Yanjie Jiang, Caining Zhang, and Zipu Li. 2017. "Intramuscular Injection of Human Umbilical Cord-Derived Mesenchymal Stem Cells Improves Cardiac Function in Dilated Cardiomyopathy Rats." Stem Cell Research & Therapy 8(1):18.

38. Meng, Xin, Jianping Li, Ming Yu, Jian Yang, Minjuan Zheng, Jinzhou Zhang, Chao Sun, Hongliang Liang, and Liwen Liu. 2018. "Transplantation of Mesenchymal Stem Cells Overexpressing IL10 Attenuates Cardiac Impairments in Rats with Myocardial Infarction." Journal of Cellular Physiology 233(1):587–95.

39. Mohamed, Eman, Ahmed Reda, and Heba Elnegris. 2020. "Role of L-Carnitine Treated Mesenchymal Stem Cells on Histological Changes in Spleen of

Experimentally Induced Diabetic Rats and the Active Role of Nrf2 Signaling." Egyptian Journal of Histology.

40. Mohamed, Sarah S., Lamiaa A. Ahmed, Wael A. Attia, and Mahmoud M. Khattab. 2015. "Nicorandil Enhances the Efficacy of Mesenchymal Stem Cell Therapy in Isoproterenol-Induced Heart Failure in Rats." Biochemical Pharmacology 98(3):403–11.

41. Mortezaee, Keywan, Parichehr Pasbakhsh, Iraj Ragerdi Kashani, Fatemeh Sabbaghziarani, Ameneh Omidi, Adib Zendedel, Soudabeh Ghasemi, and Ahmad Reza Dehpour. 2016. "Melatonin Pretreatment Enhances the Homing of Bone Marrow-Derived Mesenchymal Stem Cells Following Transplantation in a Rat Model of Liver Fibrosis." Iranian Biomedical Journal 20(4):207–16.

42. Mustafa, Zannara, Sana Ashraf, Syeda Fareeha Tauheed, and Sikandar Ali. 2017. "Monosodium Glutamate, Commercial Production, Positive and Negative Effects on Human Body and Remedies - A Review." International Journal of Scientific Research in Science and Technology 3:425–35.

43. Nascimento, Diana Santos, Diogo Mosqueira, Luís Moura Sousa, Mariana Teixeira, Mariana Filipe, Tatiana Pinho Resende, Ana Francisca Araújo, Mariana Valente, Joana Almeida, José Paulo Martins, Jorge Miguel Santos, Rita Nogueira Bárcia, Pedro Cruz, Helder Cruz, and Perpétua Pinto-do-Ó. 2014. "Human Umbilical Cord Tissue-Derived Mesenchymal Stromal Cells Attenuate Remodeling after Myocardial Infarction by Proangiogenic, Antiapoptotic, and Endogenous Cell-Activation Mechanisms." Stem Cell Research & Therapy 5(1):5.

44. Ni, Tingjuan, Na Lin, Wenqiang Lu, Zhenzhu Sun, Hui Lin, Jufang Chi, and Hangyuan Guo. 2020a. "Dihydromyricetin Prevents Diabetic Cardiomyopathy via MiR-34a Suppression by Activating Autophagy." Cardiovascular Drugs and Therapy 34(3):291–301.

45. Ni, Tingjuan, Na Lin, Wenqiang Lu, Zhenzhu Sun, Hui Lin, Jufang Chi, and Hangyuan Guo. 2020b. "Dihydromyricetin Prevents Diabetic Cardiomyopathy via MiR-34a Suppression by Activating Autophagy." Cardiovascular Drugs and Therapy 34(3):291–301.

46. Orlic, Donald, Jan Kajstura, Stefano Chimenti, Federica Limana, Igor Jakoniuk, Federico Quaini, Bernardo Nadal-Ginard, David M. Bodine, Annarosa Leri, and Piero Anversa. 2001. "Mobilized Bone Marrow Cells Repair the Infarcted Heart, Improving Function and Survival." Proceedings of the National Academy of Sciences 98(18):10344–49.

47. Pan, Yong, Yi Wang, Yunjie Zhao, Kesong Peng, Weixin Li, Yonggang Wang, Jingjing Zhang, Shanshan Zhou, Quan Liu, Xiaokun Li, Lu Cai, and Guang Liang. 2014. "Inhibition of JNK Phosphorylation by a Novel Curcumin Analog Prevents High Glucose-Induced Inflammation and Apoptosis in Cardiomyocytes and the Development of Diabetic Cardiomyopathy." Diabetes 63(10):3497–3511.

48. Quevedo, Henry C., Konstantinos E. Hatzistergos, Behzad N. Oskouei, Gary S. Feigenbaum, Jose E. Rodriguez, David Valdes, Pradip M. Pattany, Juan P. Zambrano, Qinghua Hu, Ian McNiece, Alan W. Heldman, and Joshua M. Hare. 2009. "Allogeneic Mesenchymal Stem Cells Restore Cardiac Function in Chronic Ischemic Cardiomyopathy via Trilineage Differentiating Capacity." Proceedings of the National Academy of Sciences 106(33):14022–27.

49. Ramos-Vara, José A., Matti Kiupel, Timothy Baszler, Laura Bliven, Bruce Brodersen, Brian Chelack, Stefanie Czub, Fabio Del Piero, Sharon Dial, E. J. Ehrhart, Tanya Graham, Lisa Manning, Daniel Paulsen, Victor E. Valli, Keith West, and American Association of Veterinary Laboratory Diagnosticians Subcommittee on Standardization of Immunohistochemistry. 2008. "Suggested Guidelines for Immunohistochemical Techniques in Veterinary Diagnostic Laboratories." Journal of Veterinary Diagnostic Investigation: Official Publication of the American Association of Veterinary Laboratory Diagnosticians, Inc 20(4):393–413.

50. Saberi, Kamran, Parichehr Pasbakhsh, Ameneh Omidi, Maryam Borhani-Haghighi, Saeid Nekoonam, Negar Omidi, Sodabeh Ghasemi, and Iraj Ragerdi Kashani. 2019. "Melatonin Preconditioning of Bone Marrow-Derived Mesenchymal Stem Cells Promotes Their Engraftment and Improves Renal Regeneration in a Rat Model of Chronic Kidney Disease." Journal of Molecular Histology 50(2):129–40.

51. Saini, Uksha, Richard J. Gumina, Brian Wolfe, M. Lakshmi Kuppusamy, Periannan Kuppusamy, and Konstantinos Dean Boudoulas. 2013. "Preconditioning Mesenchymal Stem Cells with Caspase Inhibition and Hyperoxia Prior to Hypoxia Exposure Increases Cell Proliferation: Preconditioning Mesenchymal Stem Cells." Journal of Cellular Biochemistry 114(11):2612–23.

52. Sanii, Sanaz, Hiva Saffar, Hedieh M. Tabriz, Mostafa Qorbani, Vahid Haghpanah, and Seyed M. Tavangar. 2012. "Expression of Matrix Metalloproteinase-2, but Not Caspase-3, Facilitates Distinction between Benign and Malignant Thyroid Follicular Neoplasms." Asian Pacific Journal of Cancer Prevention: APJCP 13(5):2175–78.

53. Sano, Toshikazu, Shuta Ishigami, Tatsuo Ito, and Shunji Sano. 2020. "Stem Cell Therapy in Heart Disease: Limitations and Future Possibilities." Acta Medica Okayama 74(3):185–90.

54. Selem, Sarah, Konstantinos E. Hatzistergos, and Joshua M. Hare. 2013. "Cardiac Stem Cells – Biology and Therapeutic Applications." Pp. 603–19 in Handbook of Stem Cells. Elsevier.

55. Sheu, Jiunn-Jye, Han-Tan Chai, Pei-Hsun Sung, John Y. Chiang, Tien-Hung Huang, Pei-Lin Shao, Shun-Cheng Wu, and Hon-Kan Yip. 2021. "Double Overexpression of MiR-19a and MiR-20a in Induced Pluripotent Stem Cell-Derived Mesenchymal Stem Cells Effectively Preserves the Left Ventricular Function in Dilated Cardiomyopathic Rat." Stem Cell Research & Therapy 12(1):371.

56. Soleimani, Masoud, and Samad Nadri. 2009. "A Protocol for Isolation and Culture of Mesenchymal Stem Cells from Mouse Bone Marrow." Nature Protocols 4(1):102–6.

57. Spezzacatene, Anita, Gianfranco Sinagra, Marco Merlo, Giulia Barbati, Sharon L. Graw, Francesca Brun, Dobromir Slavov, Andrea Di Lenarda, Ernesto E. Salcedo, Jeffrey A. Towbin, Jeffrey E. Saffitz, Frank I. Marcus, Wojciech Zareba, Matthew R. G. Taylor, Luisa Mestroni, and the Familial Cardiomyopathy Registry. 2015. "Arrhythmogenic Phenotype in Dilated Cardiomyopathy: Natural History and Predictors of Life-Threatening Arrhythmias." Journal of the American Heart Association 4(10):e002149.

58. Suvarna SK, Layton C. and Bancroft JD. 2018. Pp. 140–47 in Bancroft's Theory and Practice of Histological Techniques. ELSEVIER.

59. Tarbit, Emiri, Indu Singh, Jason N. Peart, and Roselyn B. Rose'Meyer. 2019. "Biomarkers for the Identification of Cardiac Fibroblast and Myofibroblast Cells." Heart Failure Reviews 24(1):1–15.

60. Wang, Jing, Huaide Liu, Ning Li, Quanbin Zhang, and Hong Zhang. 2014. "The Protective Effect of Fucoidan in Rats with Streptozotocin-Induced Diabetic Nephropathy." Marine Drugs 12(6):3292–3306.

61. Wenzl, Florian A., Samuele Ambrosini, Shafeeq A. Mohammed, Simon Kraler, Thomas F. Lüscher, Sarah Costantino, and Francesco Paneni. 2021. "Inflammation in Metabolic Cardiomyopathy." Frontiers in Cardiovascular Medicine 8:742178.

62. Westermann, Dirk, Sophie Van Linthout, Sameer Dhayat, Nasser Dhayat, Andre Schmidt, Michel Noutsias, Xi-Yong Song, Frank Spillmann, Alexander Riad, Heinz-Peter Schultheiss, and Carsten Tschöpe. 2007. "Tumor Necrosis Factor-Alpha Antagonism Protects from Myocardial Inflammation and Fibrosis in Experimental Diabetic Cardiomyopathy." Basic Research in Cardiology 102(6):500–507.

63. Williams, Adam R., and Joshua M. Hare. 2011. "Mesenchymal Stem Cells: Biology, Pathophysiology, Translational Findings, and Therapeutic Implications for Cardiac Disease." Circulation Research 109(8):923–40.

64. Wu, Jasmine M. F., Ying-Chang Hsueh, Hui-Ju Ch'ang, Chwan-Yau Luo, Li-Wha Wu, Hiromitsu Nakauchi, and Patrick C. H. Hsieh. 2015. "Circulating Cells Contribute to Cardiomyocyte Regeneration after Injury." Circulation Research 116(4):633–41.

65. Yang, Bo, Dewei Ye, and Yu Wang. 2013. "Caspase-3 as a Therapeutic Target for Heart Failure." Expert Opinion on Therapeutic Targets 17(3):255–63.

66. Yang, Fan, Xiangjing Yu, Ting Li, Jianjun Wu, Yajun Zhao, Jiaqi Liu, Aili Sun, Shiyun Dong, Jichao Wu, Xin Zhong, Changqing Xu, Fanghao Lu, and Weihua Zhang. 2017. "Exogenous H 2 S Regulates Endoplasmic Reticulum-Mitochondria Cross-Talk to Inhibit Apoptotic Pathways in STZ-Induced Type I Diabetes." American Journal of Physiology-Endocrinology and Metabolism 312(3):E190–203.

67. Zhang, Changyi, Guichi Zhou, Yezeng Chen, Sizheng Liu, Fen Chen, Lichun Xie, Wei Wang, Yonggang Zhang, Tianyou Wang, Xiulan Lai, and Lian Ma. 2017. "Human Umbilical Cord Mesenchymal Stem Cells Alleviate Interstitial Fibrosis and Cardiac Dysfunction in a Dilated Cardiomyopathy Rat Model by Inhibiting TNF-α and TGF-β1/ERK12/ Signaling Pathways." Molecular Medicine Reports.

68. Zhang, Lei, Wen-Yuan Ding, Zhi-Hao Wang, Meng-Xiong Tang, Feng Wang, Ya Li, Ming

Zhong, Yun Zhang, and Wei Zhang. 2016. "Early Administration of Trimetazidine Attenuates Diabetic Cardiomyopathy in Rats by Alleviating Fibrosis, Reducing Apoptosis and Enhancing Autophagy." Journal of Translational Medicine 14(1):109.

69. Zhao, Lingfei, Chenxia Hu, Ping Zhang, Hua Jiang, and Jianghua Chen. 2020. "Melatonin Preconditioning Is an Effective Strategy for Mesenchymal Stem Cell-Based Therapy for Kidney Disease." Journal of Cellular and Molecular Medicine 24(1):25–33.

70. Zhou, Long, Xi Chen, Tao Liu, Yihong Gong, Sijin Chen, Guoqing Pan, Wenguo Cui, Zong-Ping Luo, Ming Pei, Huilin Yang, and Fan He. 2015. "Melatonin Reverses H 2 O 2 -Induced Premature Senescence in Mesenchymal Stem Cells via the SIRT1-Dependent Pathway." Journal of Pineal Research 59(2):190–205.

71. Zhu, Ying, Tianrui Yang, Jinlan Duan, Ninghui Mu, and Tong Zhang. 2019. "MALAT1/MiR-15b-5p/MAPK1 Mediates Endothelial Progenitor Cells Autophagy and Affects Coronary Atherosclerotic Heart Disease via MTOR Signaling Pathway." Aging 11(4):1089–1109.

72. Emiri Tarbit & Indu Singh & Jason N. Peart & Roselyn B. Rose'Meyer. Biomarkers for the identification of cardiac fibroblast and myofibroblast cells. Heart Failure Reviews 2019; 24:1–15.

73. Mustafa Z, Ashraf S, Tauheed SF, Ali S. Monosodium glutamate, commercial production, positiveand negative effects on human body and remedies- areview. IJSRST. 2017; 3:42535-.

74. Lai R, Long Y, Li Q, Zhang X and Rong T: Oxidative stress markers may not be early markers of doxorubicin-induced cardiotoxicity in rabbits. Exp. Ther. Med. 2011; 2(5): 947- 950.

75. Chugun A, Temma K, Oyamada T, Suzuki N, Kamiya Y, Hara Y, Sasaki T, Kondo H and Akera T (2000): Doxorubicin - induced late cardiotoxicity: delayed impairment of Ca2+ - handling mechanisms in the sarcoplasmic reticulum in the rat. Can. J. Physiol. Pharmacol. 78(4): 329- 338.

76. Zhang, L., Ding, W. Y., Wang, Z. H., Tang, M. X., Wang, F., Li, Y., … Zhang, W. (2016). Early administration of trimetazidine attenuates diabetic cardiomyopathy in rats by alleviating fibrosis, reducing apoptosis and enhancing autophagy. Journal of Translational Medicine, 14(1), 1–12.